HHS Public Access

Author manuscript

IEEE SICE RSJ Int Conf Multisens Fusion Integr Intell Syst. Author manuscript; available in PMC 2016 April 26.

Published in final edited form as:

IEEE SICE RSJ Int Conf Multisens Fusion Integr Intell Syst. 2015 September ; 2015: 322–327. doi: 10.1109/MFI.2015.7295828.

Force-Based Puncture Detection and Active Position Holding for Assisted Retinal Vein Cannulation*

Berk Gonenc [Student Member, IEEE],
CISST ERC at Johns Hopkins University, Baltimore, MD 21218 USA

Nhat Tran,
CISST ERC at Johns Hopkins University, Baltimore, MD 21218 USA

Cameron N. Riviere [Senior Member, IEEE],
Robotics Institute at Carnegie Mellon University, Pittsburgh, PA 15213 USA

Peter Gehlbach [Member, IEEE],
Wilmer Eye Institute at The Johns Hopkins School of Medicine, Baltimore, MD 21287 USA

Russell H. Taylor [Fellow, IEEE], and
CISST ERC at Johns Hopkins University, Baltimore, MD 21218 USA

Iulian Iordachita [Senior Member, IEEE]
CISST ERC at Johns Hopkins University, Baltimore, MD 21218 USA

Berk Gonenc: bgonenc1@jhu.edu; Nhat Tran: ntran16@jhu.edu; Cameron N. Riviere: camr@ri.cmu.edu; Peter Gehlbach: pgelbach@jhmi.edu; Russell H. Taylor: rht@jhu.edu; Iulian Iordachita: iordachita@jhu.edu

Abstract

Retinal vein cannulation is a demanding procedure proposed to treat retinal vein occlusion by direct therapeutic agent delivery methods. Challenges in identifying the moment of venous puncture, achieving cannulation and maintaining cannulation during drug delivery currently limit the feasibility of the procedure. In this study, we respond to these problems with an assistive system combining a handheld micromanipulator, Micron, with a force-sensing microneedle. The integrated system senses the instant of vein puncture based on measured forces and the position of the needle tip. The system actively holds the cannulation device securely in the vein following cannulation and during drug delivery. Preliminary testing of the system in a dry phantom, stretched vinyl membranes, demonstrates a significant improvement in the total time the needle could be maintained stably inside of the vein. This was especially evident in smaller veins and is attributed to decreased movement of the positioned cannula following venous cannulation.

*Research supported in part by the National Institutes of Health under R01 EB007969, and R01 EB000526, and in part by Johns Hopkins University internal funds as Research to Prevent Blindness, The J. Willard and Alice S. Marriott Foundation, The Gale Trust and Mr. Bill Wilbur.

Corresponding author: Berk Gonenc, phone: 360-975-1676; bgonenc1@jhu.edu.

I. Introduction

Retinal vein occlusion (RVO) is the second most prevalent retinovascular disease affecting an estimated 16.4 million adults worldwide [1]. Retinal vein cannulation (RVC) is still an experimental surgical procedure proposed to treat RVO by direct therapeutic agent delivery methods. The procedure has historically involved the injection of clot-dissolving tissue plasminogen activator (t-PA) directly into the occluded vein [2].

Cannulation of retinal vessels has been previously explored using a variety of *in vivo* animal models previously. Prior work shows that puncturing larger vessels is technically easier than piercing the smaller veins distal to the optic nerve [3]. Nevertheless, when a small branch vein (typically Ø<200 μm) is occluded, cannulation of a nearby larger vessel instead is thought to diminish the effectiveness of the treatment [4]. Therefore fine, sharp tips of drawn glass micropipettes have been utilized to enable injection directly into such small branch retinal veins [5]. However, the transparency and fragility of small glass tips result in visibility and safety issues. As an alternative, stainless steel microneedles have been proposed [6]. Tests on porcine eyes showed feasibility, and this is further supported by successful clinical demonstrations on human retinal veins [7]. Despite this progress, visualizing the cannulating tip using the surgical microscope is not trivial. In addition, operating safely on the extremely delicate retinal tissue requires very accurate tool manipulation inside of the eye. Therefore at the present time, RVC remains at the limit of human performance.

In RVC, there are three main challenges: (1) guiding the tool tip onto the target retinal vein accurately, (2) piercing the vein wall and stopping the cannula precisely at the correct depth, and (3) holding the needle tip inside of the vessel for several minutes until the drug injection at a tolerated pressure is completed. Retinal veins are very small structures (Ø<500 μm [8]) and injection into these veins requires the use of even smaller microneedles. On the other hand, the physiological hand tremor of vitreoretinal surgeons has been measured to be over 100 μm in amplitude [9], which significantly hinders precise aiming during needle insertion as well as the ability to reliably maintain cannulation during t-PA delivery. As a remedy, teleoperated [10–12], cooperatively-controlled [13,14], and handheld [15] robotic devices were proposed. Although smooth and accurate tool motion is achieved via these systems, challenges to identifying the vessel puncture, establishing cannulation and maintaining it during drug injection persist.

Conventional venipuncture occurs on larger structures and the resulting tactile forces are both perceptible and familiar to experienced phlebotomists. Specifically the clinician can feel the moment of vessel puncture [18]. Unlike a routine venipuncture, cannulating human retinal veins occurs at forces that are almost imperceptible to humans. Tests in the chorioallantoic membrane (CAM) model using chicken embryos—an accepted *in vivo* model for human RVC studies [19]—have confirmed that most RVC forces lie below the human perception threshold, yet there is still a sharp force drop upon venous puncture, as observed in a conventional venipuncture [20]. Continuous monitoring of these small forces therefore have the potential to inform the operator of the moment of vein puncture during

RVC, thereby allowing the operator to halt needle advancement and appropriately begin drug injection minimizing damage to the delicate retinal vasculature. To provide force feedback in retinal microsurgery, we developed a family of force-sensing instruments using fiber Bragg grating (FBG) strain sensors. These tools (hook [21] and micro-forceps [22–24]) were shown to accurately measure the micro-forces directly at the tool tip without significant degradation due to varying ambient temperature or the forces at the sclerotomy port. Following a similar approach, we developed a force-sensing microneedle with a thin (Ø70 μm), easily replaceable pre-bent (45°) tip for a safe RVC without overshoot [25]. This tool was driven on a linear stage and provided auditory feedback upon sensing the event of vessel puncture. When tested on CAM, the method led to successful cannulation of very thin veins (Ø<200 μm) without significant trauma in most of the trials.

This study builds on our previous work, and combines our force-sensing microneedle with a micromanipulator, Micron. The microneedle (1) measures the tool-to-tissue interaction forces, and (2) informs the operator upon the event of vein puncture via auditory feedback. Micron (1) attenuates hand-tremor of the operator to provide a smoother and safer approach to the vein surface, and (2) holds the needle tip position fixed after venous puncture by actively compensating the unintentional movements of the operator to help maintain cannulation for a longer time. This is, to the best of our knowledge, the first handheld assistive RVC system that can detect venous puncture and act automatically.

In the following sections we will first present the design of our force-sensing tool and the associated puncture detection algorithm. Sections IV and V present experimental performance assessment using an artificial phantom. The paper concludes with a discussion of the results, current limitations and our future aims.

II. System Components

A. Force-Sensing Microneedle

Injecting t-PA into thin branch retinal veins (Ø<200 μm) requires the use of even thinner and sharper tipped cannulae. Targeting Ø100–500 μm veins, we used a microneedle with an outer diameter of 70 μm (Fig. 1). The microneedle has a sharp beveled (15°) and bent tip. If a straight microneedle were used, overshooting the target vein would be almost inevitable as the insertion forces would push the vein walls towards each other and make the already thin lumen even smaller. To avoid overshoot, it is important to approach the vein wall at an angle, and move the needle tip almost horizontally along the vein with minimal vertical motion into the vein. The optimal approach angle while cannulating the vasculature on CAM was previously studied, which revealed a range of 25–35 degrees [11]. Considering the pars plana position for tool insertion, the size of the typical adult eye, and an ideal approach of ~30°, we bent the needle tip 45° relative to the tool shaft. In order to keep the sharp and bent microneedle protected and straight while inserting it through the sclera, we devised a motorized unit, which slides the outer tube in Fig. 1a along the tool shaft as a protective sheath to hide or expose the needle tip. This actuation is independent from the site of attachment, so that the microneedle can easily be used on any of the existing assistive robots

[10–15] without interfering with their operation. The design and control mechanism of this part are further detailed in [25].

Detection of vessel puncture while cannulating retinal veins requires the use of a very sensitive force sensor with sub-mN resolution. Since the forces at the sclera insertion port can be much larger than the typical cannulation forces at the tool tip, the force sensing elements need to be located close to the tool apex and inside of the eye. FBG strain sensors (Smart Fibers, UK), with their small dimension, high sensitivity, biocompatibility, sterilizability, and immunity from electrostatic and electromagnetic noise satisfy these criteria. Sensing only the transverse loads on the tool tip is sufficient for RVC since, due to design (bent tip), forces induced on the tool tip during insertion will be mostly lateral. This feature was added by fixing 3 FBGs evenly around the protective outer tube (Fig. 1a) using medical epoxy adhesive. This results in a total tool shaft diameter less than 0.9 mm, which is sufficiently small for insertion through the sclera. The calibration setup and protocol of the force sensor follow [21]. All FBGs exhibit a linear reproducible behavior during both the x- and y-axis calibration procedures (Fig. 2a). The pseudo-inverse of the resulting calibration matrix (K^+) is used in the linear relationship (1) to compute the transverse tool tip forces (F_x and F_y) from the FBG wavelength shifts (ΔS) during the operation.

$$\begin{bmatrix} F_x \\ F_y \end{bmatrix} = K^+ \cdot \Delta S, \quad \text{where } K = \begin{bmatrix} -0.0020 & -0.0017 \\ 0.0023 & -0.0011 \\ -0.0003 & 0.0028 \end{bmatrix} \quad (1)$$

In order to measure ΔS, we use an optical sensing interrogator, sm130–700 from Micron Optics Inc. (Atlanta GA). The wavelength resolution of the interrogator is 1 pm. Based upon the obtained calibration matrix, this corresponds to a transverse force resolution of about 0.25 mN. To verify sensor operation, the tool tip was loaded and unloaded repeatedly in different angles (0°, 45° and 90°), and the computed forces were compared with the actual tip loading. The root mean square error was 0.31 mN and 0.24 mN respectively for F_x and F_y. The histogram of the residual errors (Fig. 2b) show that the probability of errors beyond 0.5 mN is very low. For 0–10 mN range, computed forces match the actual values for both F_x and F_y, producing a close fit to the ideal straight line (slope=1) passing through the origin in Fig. 2c. Above 10 mN, although F_y accuracy is preserved, F_x is observed to slightly deviate from the ideal line as the loading is increased. This is the effect of torque generated due to the distance between the tip of bent needle and the tool shaft center as illustrated in Fig. 2c. Such error can in theory be corrected by modeling the error. However during RVC, since the needle insertion will take place mostly along the needle axis (y-axis of the tool), forces exceeding 10 mN along the x-axis are highly unexpected. Thus, the slight deviation in F_x at larger amplitudes is not a major concern.

B. Handheld Micromanipulator: Micron

In order to suppress involuntary hand motion, and maintain the cannula inside the vein for a longer time while minimizing trauma to the vasculature, various robotic surgical systems can be used. Most of the existing platforms for intraocular surgery are mechanically grounded

systems [10–14]. Alternative to these approaches is a handheld micromanipulator, Micron [15,16], which preserves the intuitive feel of manual handheld tools. It is normally designed to actively attenuate the physiological hand tremor of the surgeon. The position of its handle is determined by its custom microscale optical tracking system, namely the ASAP (Apparatus to Sense Accuracy of Position) [17]. After sensing the tool motion, it is filtered into its voluntary and involuntary (tremulous) components. Then activating its 3 piezoelectric actuators, Micron moves its tip to counteract the involuntary motion component within a workspace of approximately a 1×1×0.5 mm volume centered on the handle position. The control software for this operation mode is implemented in LabVIEW, and can be altered to perform other micromanipulation goals rather than solely tremor canceling.

III. System Operation

A. Puncture Detection Algorithm

In earlier needle puncture studies using rabbit ear veins [18] and CAM of fertilized chicken eggs [20], a characteristic force behavior was reported: after the needle tip touches the vein surface, the insertion force gradually rises until a sharp drop signaling the entrance of needle tip into the vein. Our team showed the feasibility of identifying this instant based on the time derivative of measured forces, and alerting the operator via auditory feedback earlier [25]. In [25], the microneedle was driven into the target vein using a linear stage, which provided a unidirectional continuous needle motion at a fixed speed. In this case, checking only the time derivative of force was sufficient and any drop in force ($\mathrm{d}\left|\overrightarrow{\mathrm{F}}_{\mathrm{needle}}\right|/\mathrm{dt}<0$) could easily be related to a puncture event. Using a linear stage to drive the microneedle though, does not provide the necessary dexterity required while working on a real eye, which is thus replaced with Micron in this work.

Using a handheld tremor-canceling micromanipulator, it is difficult to guarantee a constant insertion speed. While pushing the needle against the vein wall, moving the tool slightly slower or backing up before puncture can cause a drop in force magnitude ($\left|\overrightarrow{\mathrm{F}}_{\mathrm{needle}}\right|$), which can be misinterpreted as a puncture event if the sensing system is checking only the time derivative of forces ($\mathrm{d}\left|\overrightarrow{\mathrm{F}}_{\mathrm{needle}}\right|/\mathrm{dt}$). To avoid this error, it is important to define a puncture detection criterion based on both the measured tool tip position ($\overrightarrow{\mathrm{p}}_{\mathrm{needle}}$) and force ($\overrightarrow{\mathrm{F}}_{\mathrm{needle}}$). When the needle tip is in contact with the vein wall, the time derivative of the sensed force normally opposes the needle velocity direction. In other words, if the needle is moved into the vein deforming but not puncturing it, the derivative of the measured reaction force will be pointing out of the vein. Upon piercing the vein, however, this vector ($\mathrm{d}\overrightarrow{\mathrm{F}}_{\mathrm{needle}}/\mathrm{dt}$) instantaneously flips its orientation and points in the same direction as the velocity vector ($\mathrm{d}\overrightarrow{\mathrm{p}}_{\mathrm{needle}}/\mathrm{dt}$). This can easily be detected by checking the inner product of the two vectors. Since the microneedle is bent 45° relative to the tool shaft, the insertion will induce mostly transverse (negligible axial) forces at the tool tip. Thus, although the force sensing properties of our microneedle are limited to only two dimensions

(F^{x}_{needle} and F^{y}_{needle}), puncture of the vein can still be captured effectively by taking $dF^{z}_{needle}/dt=0$.

B. Control Scheme

The puncture detection algorithm was integrated with the Micron software via a custom LabVIEW program to provide auditory feedback to the operator and to hold the needle tip fixed with the aid of Micron upon venous puncture. The operation mode of Micron is regulated based on the logic presented in Table I. In this control scheme (Fig. 3), the wavelength information from each FBG sensor is collected and processed at 1 kHz and transmitted over TCP/IP to the LabVIEW environment. Using the calibration matrix, the transverse force at the tool tip is obtained. Then, the time derivative of tip force is computed and passed through a second-order low-pass filter. The optimal filter parameters were tuned based on measured force profiles in [20] so that the sharp drop, thus the vessel puncture, could be detected with minimal delay. The tool tip position is acquired from the ASAP tracker at a sampling rate of 1 kHz, and the tip velocity is computed. During the needle insertion phase, Micron works in its regular tremor-canceling mode, filtering out the high frequency components of the sensed motion. When puncture is detected, an alarm sound is generated to inform the operator of the puncture event, and Micron locks its goal position to the tip position recorded at this instant (puncture position). In this mode of operation, even if the user unintentionally moves the Micron handle, Micron deflects its tip to actively compensate the motion so that the tip is held fixed right at the puncture point. This active position holding mode is functional within the limits of Micron's actuators (within a sphere of ~0.5 mm radius). Deviating from the puncture point beyond these limits will saturate the actuators, and thus may not be compensated. The operator still maintains the gross positioning control while Micron makes fine adjustments to fixate the tool tip. In this way, Micron actuation can be overridden if needed, in case the needle needs to be quickly removed from the tissue.

IV. Experiments

We performed a preliminary experimental study to quantify the effects of our system on operator performance during simulated cannulation trials. The setup (Fig. 4) was designed to replicate the main challenges of RVC, and as a very consistent platform to enable testing. To simulate the retina and its vasculature, CAM is an anatomically similar model in both scale and the composition of structure and morphology [19]. However, using CAM, it is hard to guarantee phantom consistency throughout the trials due to slight differences in the size of cannulated veins, and the anatomical variation between the eggs. To simulate the vein wall with consistent mechanical behavior, we created an artificial phantom with thin membranes by stretching a vinyl layer onto an acrylic plate with circular holes (analogous to the polydimethyl siloxane sheet used in [12]). The force required for puncturing a vinyl layer with a needle highly depends on how much it is stretched. After studying the literature on the force magnitudes needed to puncture CAM vasculature, we adjusted the stretch amount so that the puncture force is about 20–25 mN. The corresponding vinyl layer thickness was measured with a micrometer to vary within 20–25 μm. The diameter of the holes on the

acrylic plate (Ø=2.5 mm) was selected small enough to create the necessary support for a firm tensioned membrane, and large enough to prevent any collision between the plate and the microneedle during insertion. The phantom was fixed on a light pad to clearly visualize the membrane loci under a digital microscope. The microscope view was displayed on a monitor providing only the top view of the phantom to the operator as in the case of a real RVC.

Tests were done by a non-surgeon subject with no prior cannulation experience, but with extensive training on Micron system. The task in each trial was to puncture the vinyl membrane by moving the microneedle almost entirely laterally, in the direction the needle tip is pointing, and hold the needle fixed for 45 seconds after the event of puncture. Two cases were experimented by altering the operation mode of Micron: (1) only tremor canceling, and (2) active position holding. In either case, the operator was informed upon vein puncture via auditory feedback. The needle trajectory after this instant was recorded for analysis. In order to prevent significant performance degradation in time due to fatigue, tests were completed in 3 periods, each period involving a total of 8 trials (4 trials per case), with a 10 minute break between the periods. During the trials, Micron mode was altered in random order. Since each puncture causes the membrane to lose its tension locally, every new trial was done at a sufficiently distant location from the previous puncture loci. Performance assessment was based upon the recorded deviation from the point of puncture. Analyses were done by a t-test assuming unequal variance. Statistical significance was defined as $p<0.05$.

V. Results and Discussion

The measurements from a typical trial with only tremor canceling (OTC) and with active position holding (APH) are shown in Fig. 5. In all trials, after the microneedle touched the membrane surface (the simulated vein wall), a gradual rise in force was observed. Most of the forces were exerted along the y-axis (all of the measured x-axis forces were below 3 mN) since the insertion was performed by moving the tool mostly laterally along the needle axis (y-axis) (Fig. 5b). The puncture force was 23.47±2.79 mN with OTC, and 23.24±2.67 mN with APH, revealing no statistically significant difference ($p=0.83$) between the mechanical behavior of membranes used in either case. The event of puncture was successfully detected from the sharp positive peak in the inner product of needle velocity and force variation vectors (Fig. 5c). Throughout the 45-second period following this instant, the difference in tool tip travel between OTC and APH trials is clearly visible in Fig. 5b. In OTC, all components of the position vector fluctuated, especially the z-component due to operator's poor depth perception with the provided 2D microscope view. Using APH, the tool motion after the puncture was significantly lowered. The reduced deviation from the puncture point with APH can clearly be seen in Fig. 5.d, which includes the needle tip trajectories recorded during 3 sample trials of each operation mode.

In order to assess the ability to maintain cannulation in veins of different sizes, using the measured tool tip position throughout the entire hold time (45 seconds), we computed the time spent inside five different zones with varying distance from the puncture point (Fig.

5.d). The size of each zone represents a vein diameter, and was decided based upon the typical vein sizes encountered in RVC (Ø 100–500 μm). The results (Fig. 6) show that, compared with the OTC trials, using APH enabled the operator to maintain the tip within the zone (thus the vein) for a significantly longer time for veins up to 300 μm ($p<0.05$). For instance, with OTC, the average time that the tip was maintained within a 100 μm distance from the puncture point was measured to be only 5.41 seconds with a peak value of 22.08 seconds out of the 45 second total test duration. In none of the 12 OTC trials could this duration exceed 40 seconds. However, upon using APH, the mean time was raised to 13.27 seconds, with 2 trials reaching a hold time over 40 seconds. Similar performance improvement with APH was observed in the 200 and 300 μm zones. For the 400 and 500 μm zones, in terms of the average time maintained inside, no statistically significant difference between OTC and APH could be identified ($p=0.07$ for 400 μm, $p=0.26$ for 500 μm). However, even for the 500 μm zone, where the performance of OTC and APH is closest, the number of trials with successful “in-zone” hold time over 40 seconds was still 50% greater in APH than OTC.

Our second performance metric was based on the range of needle tip travel after puncture—which needs to be minimized to reduce trauma—as a function of the hold time. For this, we analyzed the tip deviation during the first 15, 30 and 45 seconds after the puncture. The results are shown in Fig. 7. Accordingly, the almost linear rise in the maximum and mean tip travel as the needle is held for longer periods was inevitable, regardless of whether OTC or APH was used. Nevertheless, for all hold times, when APH was used, both the mean and the maximum distance from the puncture point was significantly lowered ($p<0.05$). In case of a 15-second hold time, the mean tip travel was reduced by more than 65% (from 276.18 μm to 90.34 μm). The decay was similar for the 30 and 45-second hold periods. The mean deviation from the puncture point during a 45-second hold exceeded 350 μm with OTC, whereas APH lowered it to below 200 μm, which shows that APH can potentially enable the cannulation of smaller veins, and provide an extended period of intravenous cannula stability, potentially sufficient to allow sustained periods of drug delivery at tolerable pressures.

VI. Conclusions

This work reported on the development of an assistive system combining a handheld micromanipulator with a force-sensing microneedle. The system helped the operator detect the instant of puncture during RVC, and maintain cannulation for a longer period by actively holding the microneedle tip fixed inside the vein. The event of puncture was sensed by continuously tracking the inner product of needle tip velocity and force derivative vectors. Our preliminary experimental study using artificial phantoms, stretched vinyl membranes, have shown that the proposed puncture detection algorithm combined with active positive holding can maintain the needle tip inside the vein for a much longer time especially for smaller veins, and that it significantly attenuates the tool motion in the vein following venipuncture and cannulation.

The system described in this work employed an existing handheld micromanipulator for "active" tremor canceling and position holding purposes. The operation principle is easily integrable with the other existing cooperatively-controlled or teleoperated assistive devices to provide "passive" position holding instead. Whilst a handheld device like Micron may be preferable to more experienced and skilled operators, the grounded robotic systems with their larger range of motion can potentially be a better option for novice users to learn and execute demanding tasks such as RVC. Our current work focuses on implementing this technology onto a cooperatively-controlled robot and conducting a multi-user study using *in vivo* CAM models.

References

1. Rogers S, McIntosh RL, Cheung N, Lim L, Wang JJ, Mitchell P, Kowalski JW, Nguyen H, Wong TY. The prevalence of retinal vein occlusion: Pooled data from population studies from the United States, Europe, Asia, and Australia. Ophthalmology. Feb; 2010 117(2):313–19.e1. [PubMed: 20022117]
2. Weiss JN, Bynoe LA. Injection of tissue plasminogen activator into a branch retinal vein in eyes with central vein occlusion. Ophthalmology. Jul; 2001 108(12):2249–2257. [PubMed: 11733266]
3. Tsilimbaris MK, Lit ES, D'Amico DJ. Retinal microvascular surgery: A feasibility study. Invest Ophthalmol Vis Sci. Jun; 2004 45(6):1963–1968. [PubMed: 15161864]
4. Weiss, JN. Apparatus and method for cannulating retinal blood vessels. US Patent. 6 402 734 B1. Jun 11. 2002
5. Glucksberg MR, Dunn R, Giebs CP. In vivo micropuncture of retinal vessels. Graefe's Archive for Clinical and Experimental Ophthalmology. Jul; 1993 231(7):405–407.
6. Kadonosono K, Arakawa A, Yamane S, Uchio E, Yanagi Y. An experimental study of retinal endovascular surgery wih a fabricated needle. Invest Opthalmol Vis Sci. Jul; 2011 52(8):5790–5793.
7. Kadonosono K, Yamane S, Arakawa A, Inoue M, Yamakawa T, Uchio E, Yanagi Y, Amano S. Endovascular cannulation with a microneedle for central retinal vein occlusion. JAMA Ophthalmol. Jun; 2013 131(6):783–786. [PubMed: 23764703]
8. Skovborg F, Nielsen V, Lauritzen E, Hartkopp O. Diameters of the retinal vessels in diabetic and normal subjects. Diabetes. May; 1969 18(5):292–298. [PubMed: 5795853]
9. Singh, SPN.; Riviere, CN. Physiological tremor amplitude during retinal microsurgery. Proc IEEE 28th Annu Northeast Bioeng Conf; Philadelphia. 2002. p. 171-172.
10. Jensen PS, Grace KW, Attariwala R, Colgate JE, Glucksberg MR. Toward robot-assisted vascular in the retina. Graefe's Arch Clin Exp Ophthalmol. Nov; 1997 235(11):696–701. [PubMed: 9407227]
11. Wei W, Popplewell C, Chang S, Fine HF, Simaan N. Enabling technology for microvascular stenting in ophthalmic surgery. Journal of Medical Devices. Mar.2010 4(1)
12. Tanaka S, et al. Quantitative assessment of manual and robotic microcannulation for eye surgery using new eye model. Int J Med Robotics Comput Assist Surg. Apr.2014
13. Fleming I, Balicki M, Koo J, Iordachita I, Mitchell B, Handa J, Hager G, Taylor R. Cooperative robot assistant for retinal microsurgery. Med Image Comput Comput Assist Interv. 2008; 5242:543–550. [PubMed: 18982647]
14. Gijbels, A.; Wouters, N.; Stalmans, P.; Van Brussel, H.; Reynaerts, D.; Vander Poorten, E. Design and realisation of a novel robotic manipulator for retinal surgery. Proc IEEE Int Conf on Intelligent Robots and Systems; Tokyo. 2013. p. 3598-3603.
15. Becker, BC.; Yang, S.; MacLachlan, RA.; Riviere, CN. Towards vision-based control of a handheld micromanipulator for retinal cannulation in an eyeball phantom. Proc 4th IEEE RAS EMBS Int Conf Biomed Robot Biomechatron; Rome. 2012. p. 44-49.

16. Becker BC, MacLachlan RA, Lobes LA, Hager GD, Riviere CN. Vision-based control of a handheld surgical micromanipulator with virtual fixtures. IEEE Trans Robotics. Jun; 2013 29(3): 674–683. [PubMed: 24639624]

17. MacLachlan RA, Riviere CN. High-speed microscale optical tracking using digital frequency-domain multiplexing. IEEE Trans Instrumentation and Measurement. Jun; 2009 58(9):1991–2001.

18. Saito H, Togawa T. Detection of needle puncture to blood vessel using puncture force measurement. Med Biol Eng Comput. Mar; 2005 43(2):240–244. [PubMed: 15865134]

19. Leng T, Miller JM, Bilbao KV, Palanker DV, Huie P, Blumenkranz MS. The chick chorioallantoic membrane as a model tissue for surgical retinal research and simulation. Retina. Jun; 2004 24(3): 427–434. [PubMed: 15187666]

20. Ergeneman O, Pokki J, Pocepcova V, Hall H, Abbott JJ, Nelson BJ. Characterization of puncture forces for retinal vein cannulation. J Med Dev. Dec.2011 5(4):044504.

21. Iordachita I, Sun Z, Balicki M, Kang J, Phee S, Handa J, Gehlbach P, Taylor R. A sub-millimetric, 0.25 mn resolution fully integrated fiber-optic force-sensing tool for retinal microsurgery. Int J Comput Assist Radiol Surg. Jun; 2009 4(4):383–390. [PubMed: 20033585]

22. Kuru, I.; Gonenc, B.; Balicki, M.; Handa, J.; Gehlbach, P.; Taylor, RH.; Iordachita, I. Force Sensing Micro-Forceps for Robot Assisted Retinal Surgery. Proc International Conference of the IEEE EMBS; San Diego. 2012. p. 1401-1404.

23. Gonenc, B.; Handa, J.; Gehlbach, P.; Taylor, RH.; Iordachita, I. Design of 3-DOF Force Sensing Micro-Forceps for Robot Assisted Vitreoretinal Surgery. Proc International Conference of the IEEE EMBS; Osaka. 2013. p. 5686-5689.

24. Gonenc, B.; Gehlbach, P.; Handa, J.; Taylor, RH.; Iordachita, I. Motorized Force-Sensing Micro-Forceps with Tremor Cancelling and Controlled Micro-Vibrations for Easier Membrane Peeling. Proc IEEE RAS EMBS Int Conf Biomed Robot Biomechatron; Sao Paulo. 2014. p. 244-251.

25. Gonenc, B.; Gehlbach, P.; Handa, J.; Taylor, RH.; Iordachita, I. Force-Sensing Microneedle for Assisted Retinal Vein Cannulation. Proc IEEE SENSORS; Valencia. 2014. p. 698-701.

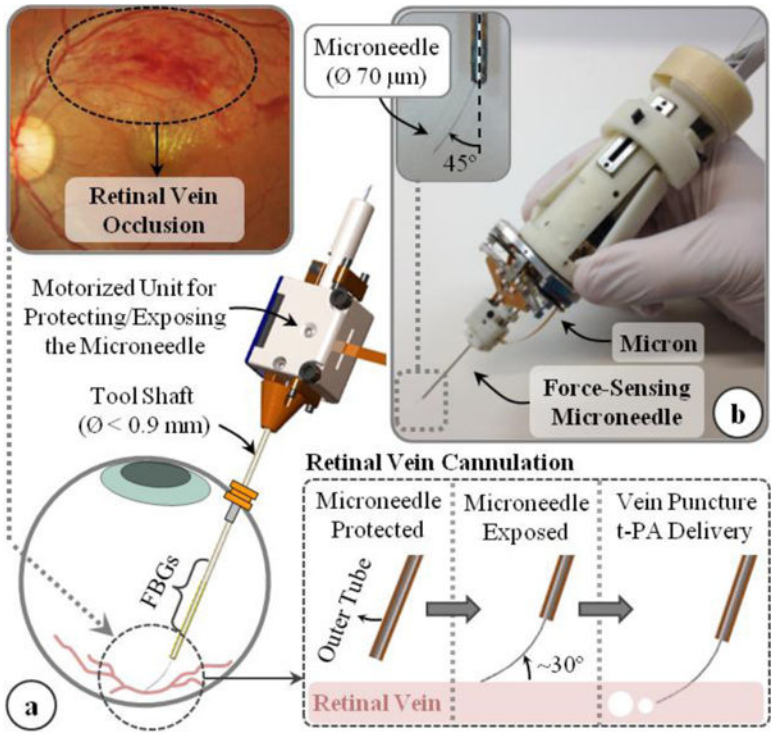

Figure 1.

(a) Conceptual overview to assist retinal vein cannulation. A microneedle is used to inject t-PA into the ocluded retinal vein. The needle is bent (45°) to approach the vein at the optimal angle (~30°). The needle is kept straight and protected inside an outer tube while inserting through the sclera. It is exposed upon reaching the vein surface via a motorized unit [25]. FBGs integrated on the tool shaft sense tool-to-tissue forces inside of the eye. (b) Fabricated prototype. The force-sensing microneedle was combined with a handheld micromanipulator, Micron.

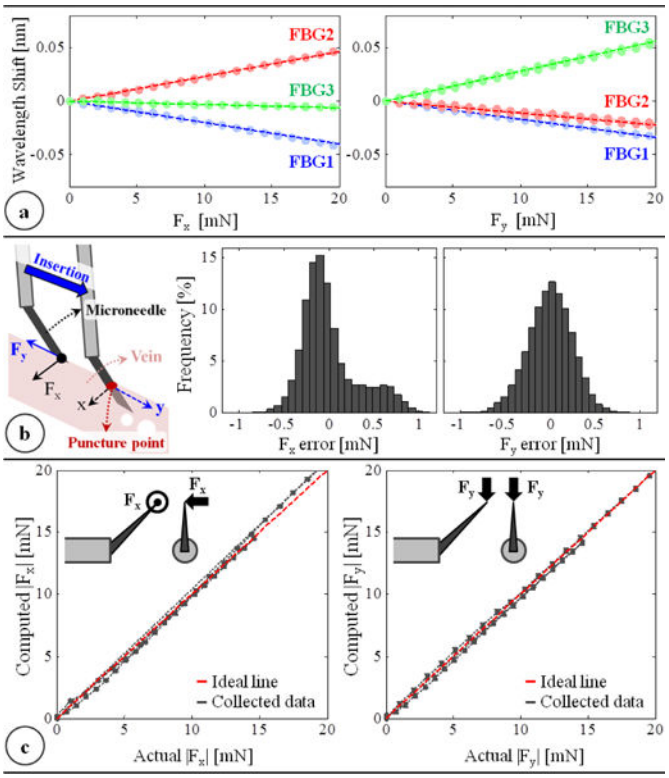

Figure 2.

(a) Calibration results: linear response for all FBGs when the needle is loaded along x and y axes. (b) The force-sensing coordinates relative to the target vein and the histogram of residual errors in each direction. (c) Computed forces vs. the actual forces along the x and y axes.

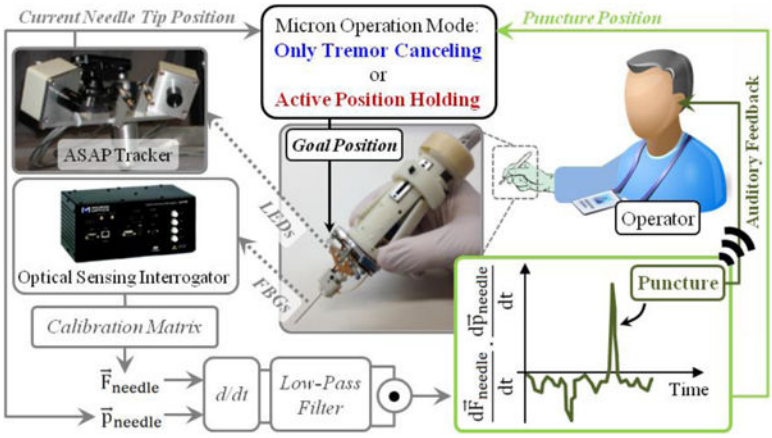

Figure 3.

The control scheme of the integrated system. The time derivative of needle position and force are computed and filtered. The inner product of the two turns positive at the event of vein puncture. When puncture is detected (1) the operator is informed with an alarm sound, and (2) Micron operation mode is switched from default “only tremor canceling” to “active position holding”.

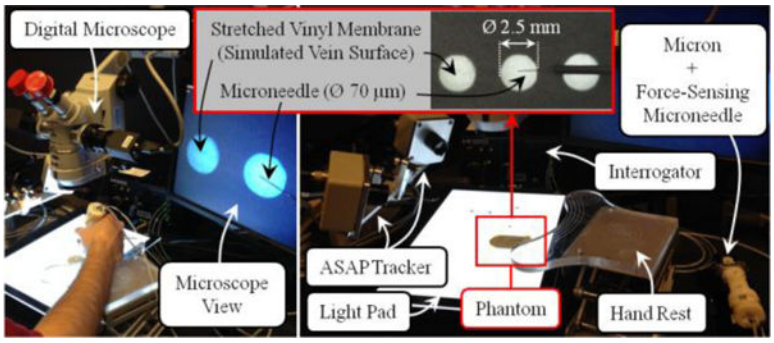

Figure 4.

The experimental setup for evaluating the performance of the developed system on an artificial phantom. Stretched vinyl membranes, simulating the vein walls, were punctured open-sky using Micron and the force-sensing microneedle.

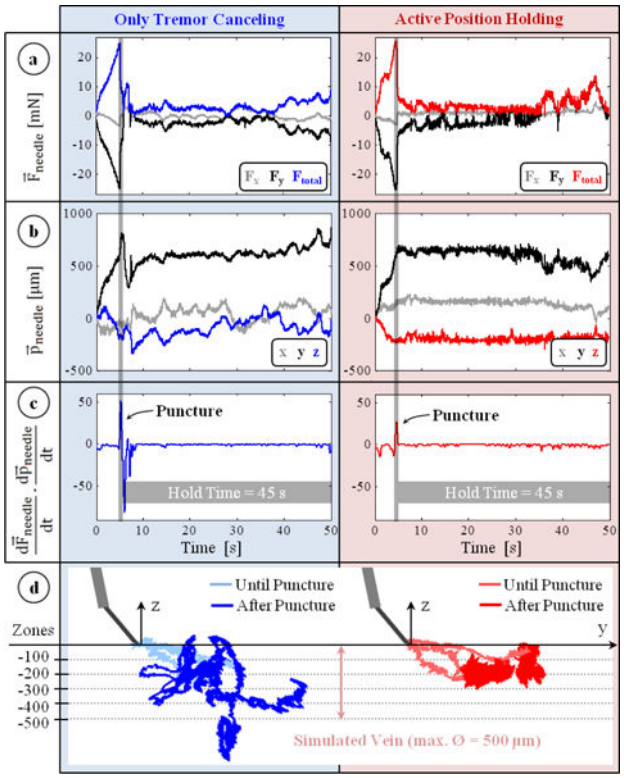

Figure 5.

Typical measurements taken during trials with only tremor canceling (blue) and active position holding (red). (a) Forces on the needle: mostly along the y-axis with a gradual rise during insertion and a sharp drop at the instant of puncture. (b) Position of the needle : remains fixed with active position holding in contrast to the fluctuations with only tremor canceling. (c) The event of puncture: a positive peak in the inner product of needle velocity and force variation vectors. (d) Recorded needle tip trajectories for 3 representative trials of each mode. Active position holding significantly reduced tool tip deviation from the puncture point.

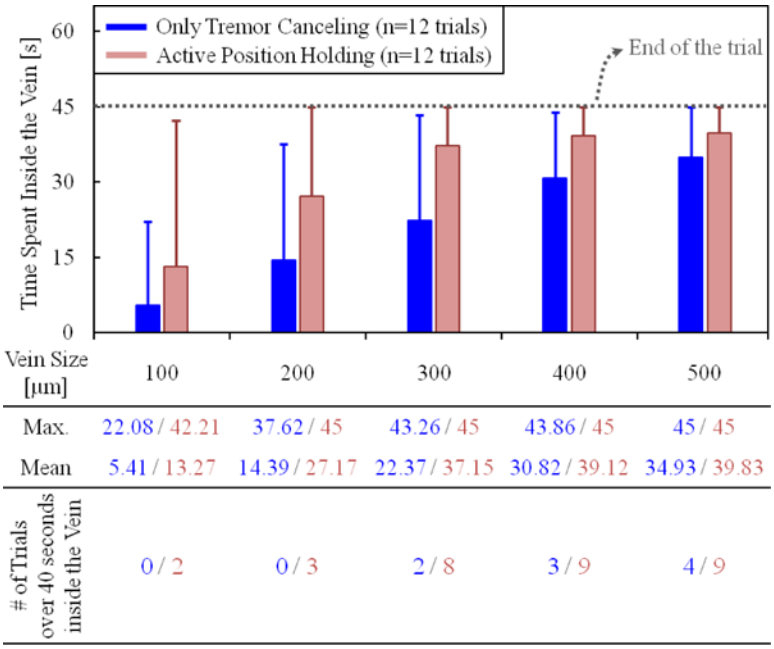

Vein Size [µm]	100	200	300	400	500
Max.	22.08 / 42.21	37.62 / 45	43.26 / 45	43.86 / 45	45 / 45
Mean	5.41 / 13.27	14.39 / 27.17	22.37 / 37.15	30.82 / 39.12	34.93 / 39.83
# of Trials over 40 seconds inside the Vein	0 / 2	0 / 3	2 / 8	3 / 9	4 / 9

Figure 6.

The total time that the needle tip was maintained inside the vein vs. the vein size. The solid bars show the mean, and the error bars represent the maximum value. The active position holding helps in maintaining the needle tip inside the vein for a significantly longer time, especially for veins smaller than 300 µm.

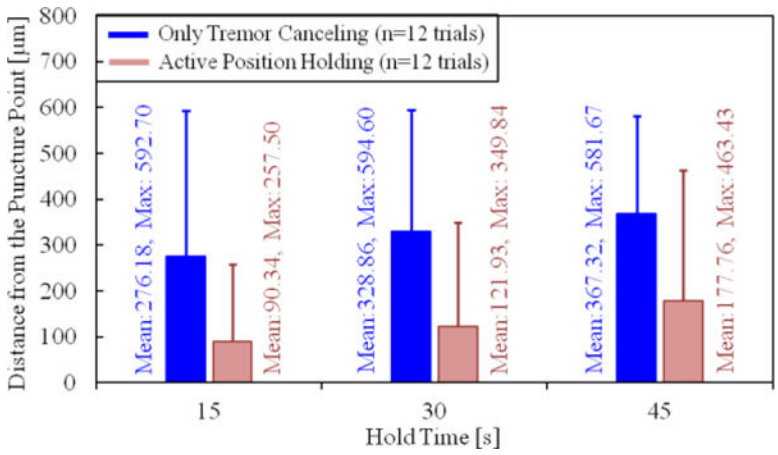

Figure 7.

Deviation from the puncture point vs. the hold time. The solid bars show the mean distance from the puncture point, and the error bars represent the maximum value. A longer hold time causes the needle to move away from the puncture point more. The active position holding significantly helps in keeping the needle tip proximal to the puncture point.

Table I

MICRON MODE REGULATION LOGIC

Condition	Puncture?	Operation Mode
$\frac{d\overrightarrow{F}_{needle}}{dt} \cdot \frac{d\overrightarrow{p}_{needle}}{dt} \leq 0$	No	Only Tremor Canceling
$\frac{d\overrightarrow{F}_{needle}}{dt} \cdot \frac{d\overrightarrow{p}_{needle}}{dt} > 0$	Yes	Active Position Holding